A Method for Calculating Iron Loss of an SR Motor Based on Reluctance Network Analysis and Comparison of Symmetric and Asymmetric Excitation

Kenji Nakamura, Shinya Fujio, and Osamu Ichinokura

Graduate School of Engineering, Tohoku University, Sendai 980-8579, Japan

This paper presents a reluctance network analysis (RNA) model of a switched reluctance motor considering iron loss. The proposed RNA model consists of a multiple number of nonlinear reluctances and magnetic inductances that express magnetic hysteresis. The validity of the proposed model is proved by comparing calculated values with measured ones. Furthermore, differences between symmetric and asymmetric excitation are investigated.

Index Terms—Electromagnetic and motion coupled analysis, iron loss, reluctance network analysis (RNA), switched reluctance (SR) motor.

I. INTRODUCTION

A SWITCHED reluctance (SR) motor has desirable features such as simple construction, high reliability, and low cost. In addition, the advancement of power electronics technology has made the SR motor more useful [1]. Now, the SR motor is applied to electric washing machines, vacuum cleaners, electric bicycles, and vehicles. It is expected that the application of the SR motor will increase in the future.

Several papers have reported on the analysis and design of SR motors. Most of the papers, however, discuss only static characteristics based on a finite element method (FEM). In the case of the SR motor, characteristics of the motor strongly depend on an excitation phase. Therefore, dynamic analysis including a motor drive circuit is necessary. Although the FEM-based electromagnetic and motion coupled analysis is being examined, its calculation time tends to be long.

Utilization of a magnetic circuit method is one of the practical solutions that aid the optimization of a motor drive system [2], [3]. Previously, we proposed a reluctance network analysis (RNA) model of an SR motor [4], which consists of a multiple number of nonlinear reluctances and magnetomotive forces (MMFs). By combining the RNA model with the motor drive circuit and motion calculation circuits, the RNA-based electromagnetic and motion coupled analysis was realized. On the other hand, a method for calculating iron loss characteristics has not been examined.

In this paper, an improved RNA model considering the iron loss is presented. Furthermore, a proper excitation direction for a 6/4-pole SR motor is investigated.

II. RNA MODEL OF SR MOTOR AND COUPLED ANALYSIS

Fig. 1 shows a schematic diagram of the 6/4-pole SR motor used in the consideration. The core material is nonoriented sil-

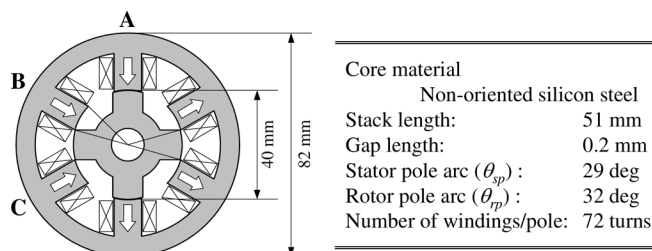| Core material	
	Non-oriented silicon steel
Stack length:	51 mm
Gap length:	0.2 mm
Stator pole arc (θ_{sp}) :	29 deg
Rotor pole arc (θ_{rp}) :	32 deg
Number of windings/pole:	72 turns

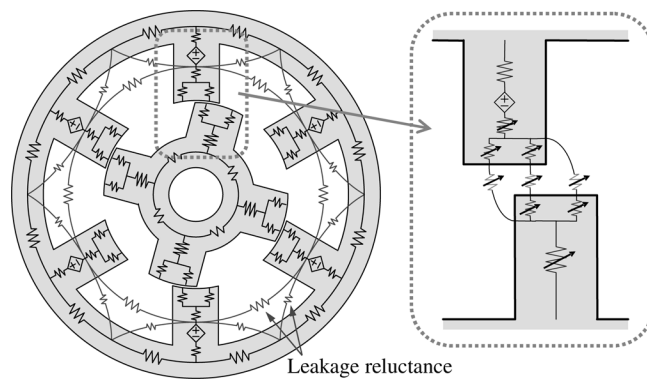Fig. 1.   Schematic diagram of the 6/4-pole SR motor.

Fig. 2.   RNA model of the 6/4-pole SR motor.

icon steel with a thickness of 0.35 mm. In the figure, the arrows indicate a direction of excitation.

Fig. 2 illustrates the RNA model of the SR motor [4]. In the model, the nonlinear reluctances in the motor core are determined based on the following equation:

$$f_m = R_m \phi = \left(\frac{\alpha_1 l}{S} + \frac{\alpha_{15} l}{S^{15}} \phi^{14} \right) \phi \qquad (1)$$

where a cross-section and length of a magnetic path are S and l, respectively. The coefficients α_1 and α_{15} are 103.26 and 1.5153, which are obtained from $B - H$ curve of the core material.
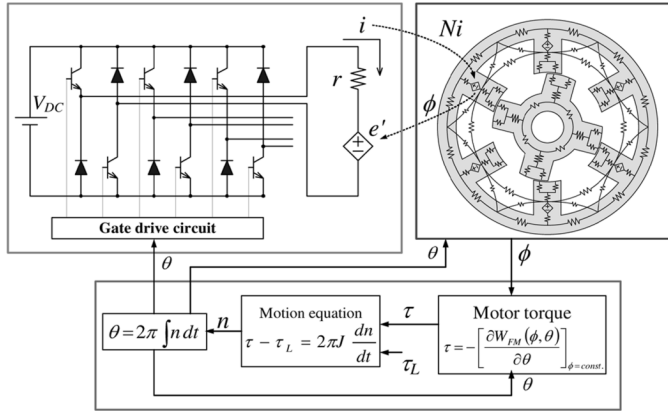
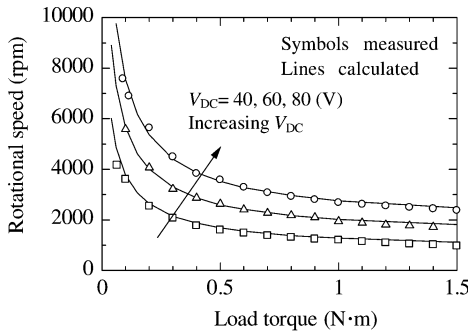Fig. 3. Electromagnetic and motion coupled analysis model of the SR motor.

Fig. 4. Rotational speed versus torque characteristics.

Fig. 5. Calculated flux density waveforms at each part of the SR motor.

Fig. 6. Iron loss curves corresponding to the distorted waveform.

The MMFs generated by winding currents are expressed in the controlled sources.

Since a flux distribution around a stator and rotor poles dynamically changes with a rotor position due to a salient pole structure, the magnetic circuit of the poles is expressed by nine variable reluctances as shown in Fig. 2. Furthermore, leakage fluxes from a stator pole are considered by using the leakage reluctances as shown in the figure.

Fig. 3 illustrates the electromagnetic and motion coupled analysis model of the SR motor. The proposed coupled model consists of three different blocks, that is, the motor drive circuit, the RNA model of the SR motor, and the motion calculation circuits. By using the coupled analysis model, characteristics of the SR motor, including the transient state, can be calculated [4].

Fig. 4 shows the rotational speed versus torque characteristics. It reveals that the calculated values agree well with the measured ones. Fig. 5 shows the calculated flux density waveforms at each part of the SR motor. In the figure, the lines are the values calculated by the RNA, and the symbols are obtained from the FEM. It is understood that both calculated values almost agree.

III. RNA MODEL TAKING ACCOUNT OF IRON LOSS

In order to estimate the iron loss characteristics, it is necessary to express the behavior of magnetic hysteresis in the RNA model. When the magnetic hysteresis is considered, a relation between MMF f_m and flux ϕ is represented by the following equation:

$$f_m = \left(\frac{\alpha_1 l}{S} + \frac{\alpha_{15} l}{S^{15}} \phi^{14} \right) \phi + \frac{\beta_1 l}{S} \frac{d\phi}{dt}. \qquad (2)$$
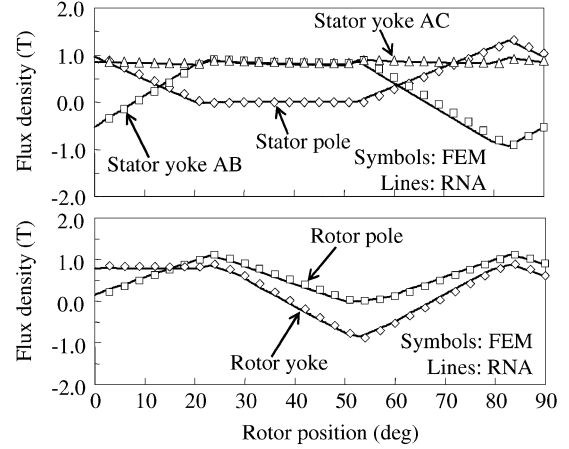
Equation (2) indicates that a magnetic circuit considering the magnetic hysteresis is composed of the nonlinear reluctance and the magnetic inductance [5]. The coefficient β_1 is determined from an iron loss curve of the core material, which is measured generally under sinusoidal excitation. On the other hand, in case the flux density is not a sinusoidal wave shown in Fig. 5, it is necessary to derive β_1 while taking into consideration the influence of harmonic distortion. In this paper, the coefficient β_1 is found according to the following procedures.

First of all, the flux density waveform with a certain amplitude is expressed in a Fourier series. The iron loss caused by the kth harmonic flux can be obtained as follows:

$$w_{\mathrm{ki}} = A_h k f B_{\mathrm{km}}^n + A_e (kf)^2 B_{\mathrm{km}}^2 \qquad (3)$$

where the hysteresis and eddy current loss coefficients are A_h and A_e, respectively. The fundamental frequency is f, and the maximum value of the kth harmonic flux density is B_{km}. The calculation assumes that the whole iron loss W_i is given by the sum of all the harmonic iron losses w_{ki} [6]. By calculating the iron loss W_i of the flux density with various amplitude, the iron loss curve according to the distorted waveform can be obtained.

Fig. 6 shows the iron loss curves corresponding to the wave forms at the stator and rotor poles when a rotational speed is 3300 rpm. The coefficient β_1 is determined from the iron loss curve. Fig. 7 shows the coefficients β_1 versus frequency characteristics. It reveals that the coefficients β_1 are inversely as the frequency.

Fig. 8 illustrates the improved RNA model of the SR motor considering the iron loss. As shown in the figure, the magnetic inductances that express the magnetic hysteresis are inserted in each part of the magnetic circuit.
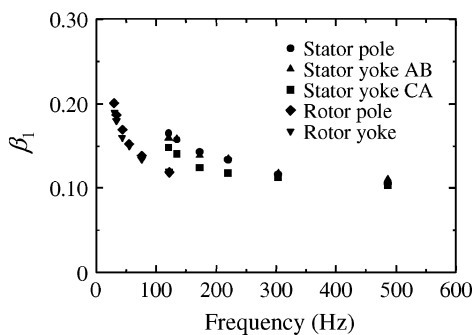
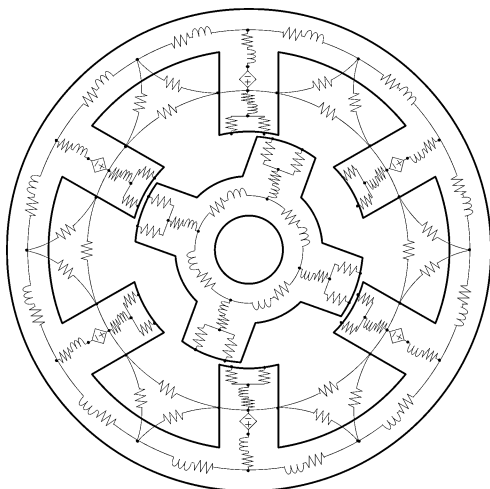Fig. 7.   Coefficient β_1 versus frequency characteristics.

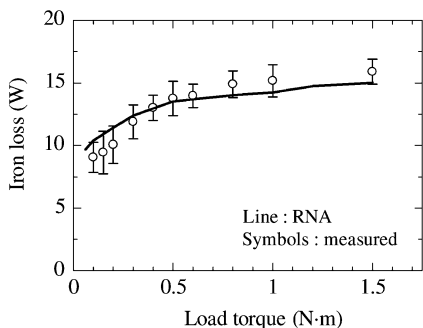Fig. 8.   RNA model of the SR motor considering iron loss.

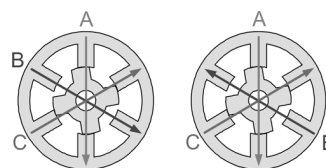Fig. 9.   Iron loss versus torque characteristics.

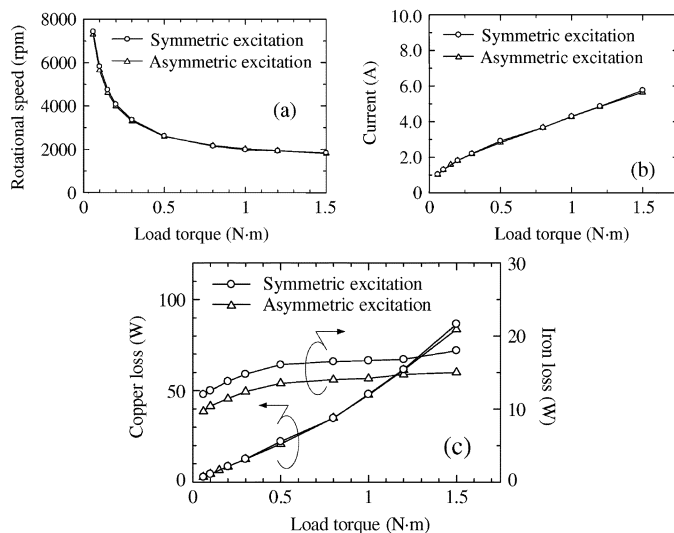Fig. 10.   Asymmetric (left) and symmetric (right) excitation.

Fig. 11.   Calculated characteristics of the SR motor with symmetric and asymmetric excitation; (a) is rotational speed, (b) is current characteristics, and (c) is loss characteristics.

Fig. 9 shows the calculated and measured iron loss characteristics of the SR motor when an exciting voltage is 60 V. In the figure, the scatter of measured values is expressed by the error bar. From the figure, it is understood that the calculated and measured values almost agree.

Since an asymmetric half bridge converter is generally used for driving SR motors, there are two directions of excitation in the case of the 6/4-pole SR motor as shown in Fig. 10. Differences between the symmetric and asymmetric excitation are investigated by using the improved RNA model.

Fig. 11 shows the calculated characteristics of the SR motor. From the figures, it is understood that the rotational speed and current characteristics are almost the same. On the other hand, the iron loss of the asymmetric excitation is smaller than that of the symmetric one, because the flux density waveforms of the both excitation are different from each other.

IV. CONCLUSION

This paper presented the RNA model of the SR motor considering the iron loss. The validity of the proposed model was proved by comparing with the measured values. The asymmetric excitation is more suitable for driving the 6/4-pole SR motor.

REFERENCES

[1] R. C. Becerra, M. Ehsani, and T. J. E. Miller, "Commutation of SR motors," *IEEE Trans. Power Electron.*, vol. 8, no. 3, pp. 257–263, Jul. 1993.
[2] H. B. Ertan, "Prediction of torque and inductance displacement characteristics of asymmetrically slotted variable-reluctance motors using a simplified model for numerical field solution," *IEEE Trans. Magn.*, vol. 35, no. 5, pp. 4247–4258, Sep. 1999.
[3] J. M. Kokernak and D. A. Torrey, "Magnetic circuit model for the mutually coupled switched-reluctance machine," *IEEE Trans. Magn.*, vol. 36, no. 2, pp. 500–507, Mar. 2000.
[4] K. Nakamura, K. Kimura, and O. Ichinokura, "Electromagnetic and motion coupled analysis for switched reluctance motor based on reluctance network analysis," *J. Magn. Magn. Mater.*, vol. 290–291, pp. 1309–1312, 2005.
[5] K. Nakamura, S. Hayakawa, S. Akatsuka, T. Ohinata, K. Minazawa, and O. Ichinokura, "Three-dimensional reluctance network analysis considering an iron loss characteristic for an EIE-core variable inductor," *IEEE Trans. Magn.*, vol. 41, no. 10, pp. 4033–4035, Oct. 2005.
[6] H. Domeki, Y. Ishihara, C. Kaido, Y. Kawase, S. Kitamura, T. Shimomura, N. Takahashi, T. Yamada, and K. Yamazaki, "Investigation of benchmark model for estimating iron loss in rotating machine," *IEEE Trans. Magn.*, vol. 40, no. 2, pp. 794–797, Mar. 2004.